Rapid Identification of Calcium Aluminate Inclusions in Steels Using Cathodoluminescence Analysis

doi: 10.1007/s11663-018-1362-0

Rapid Identification of Calcium Aluminate Inclusions in Steels Using Cathodoluminescence Analysis

Susumu Imashuku,* and Kazuaki Wagatsuma

Institute for Materials Research, Tohoku University, 2-1-1 Katahira, Aoba-ku, Sendai 980-8577, Japan

*Corresponding author: Susumu Imashuku
E-mail: susumu.imashuku@imr.tohoku.ac.jp
Telephone: +81-22-215-2132
Address: Institute for Materials Research, Tohoku University, 2-1-1 Katahira, Aoba-ku, Sendai 980-8577, Japan

ABSTRACT

We propose a method to identify calcium aluminate inclusions in calcium treated aluminum-killed steels ($Ca_{12}Al_{14}O_{33}$, $CaAl_4O_7$, $CaAl_{12}O_{19}$, and Al_2O_3) using cathodoluminescence (CL) analysis. Such inclusions result in nozzle clogging and melting of the stopper rod during continuous casting. We obtain CL images and CL spectra of calcium aluminate inclusions in model samples of calcium treated aluminum-killed steel. The model samples are prepared by heating mixtures of Fe powder, Al powder, and Ca shot at 1550 °C in an argon atmosphere. On the basis of the CL colors and CL spectra of the calcium aluminate inclusions, we demonstrate that it is possible to distinguish $Ca_{12}Al_{14}O_{33}$, $CaAl_4O_7$, $CaAl_{12}O_{19}$, and Al_2O_3 inclusions from $CaAl_2O_4$ and $Ca_3Al_{10}O_{18}$ inclusions, which do not cause nozzle clogging and melting of the stopper rod, by comparing CL images obtained using digital cameras with and without a built-in filter. The acquisition times for the CL images are less than 10 s. Thus, the method we present here can be applied for the rapid detection of harmful calcium aluminate inclusions during continuous casting. The CL spectra also provide basic information to specify compositions in agglomerated calcium aluminate inclusions.

I. INTRODUCTION

It is of vital importance to analyze nonmetallic inclusions in steels, such as alumina (Al_2O_3), spinel ($MgAl_2O_4$), silica (SiO_2), manganese sulfide (MnS), calcium sulfide (CaS), boron nitride (BN), and titanium nitride (TiN) because they can cause serious problems to steel products, such as breakage of steel wire during drawing, hydrogen induced cracking, fatigue failure, surface flaws, and low temperature embrittlement.[1-4] Such inclusions may also be problematic for the steel production process. For example, Al_2O_3 inclusions can lead to nozzle clogging in the continuous casting of aluminum (Al) killed steel (Fig. 1)[1,2,4] because Al_2O_3 solidifies at the casting temperature. Al_2O_3 inclusions are formed by Al deoxidation, which is a process to reduce the oxygen content in steel by adding aluminum metal into molten steel in the ladle (Fig. 1). To prevent nozzle clogging, calcium (Ca) is injected into the molten steel in the forms of Ca metal, ferrocalcium, Ca-Si alloy, or Mg-Ca alloy, which is termed as Ca treatment. Ca treatment is effective because solid Al_2O_3 inclusions transform into liquid calcium aluminates, which do not clog the nozzle, at the casting temperature.[5-7] However, the addition of excess Ca causes the stopper rod, which controls the flow rate of the molten steel into the mold (Fig. 1), to melt because the stopper rod is normally made from alumina-graphite.[8-10] It has been reported that the compositions of the calcium aluminate inclusions in Ca treated Al-killed steels have to be $CaAl_2O_4$ and $Ca_3Al_{10}O_{18}$ to prevent both nozzle clogging and melting of the stopper rod.[9,10] Therefore, we can detect the symptoms of nozzle clogging and melting of the stopper rod by the compositional analysis of the calcium aluminate inclusions in the steels.

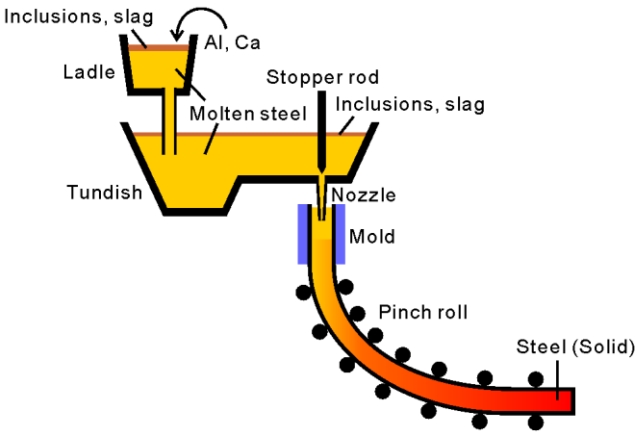

Fig. 1–Schematic illustration of a continuous casting machine.

The compositional analysis of nonmetallic inclusions in steels is usually performed using electron probe microanalyzers (EPMA).[11] This analytical process is a time-consuming step in steelmaking[2,3] because it takes approximately 1 week to complete the analysis for a single sample. Analytical techniques, such as optical emission spectrometry with pulse distribution analysis (OES-PDA),[12,13] electron beam (EB) melting,[14] cold crucible-X-ray fluorescence,[15,16] fractional thermal decomposition (FTD),[17] laser-induced breakdown spectroscopy (LIBS),[18] and cathodoluminescence analysis,[19,20] have been proposed for the rapid compositional analysis of nonmetallic inclusions in steels.[21] Among these techniques, we have recently focused on CL analysis[22-25] because CL analysis can simultaneously identify the size, shape, and composition of non-metallic inclusions, which are essential for the analysis of nonmetallic inclusions in steels. We have previously demonstrated that obtaining CL images and CL spectra enables $MgAl_2O_4$ spinel, Al_2O_3, BN, and aluminum nitride (AlN) inclusions to be distinguished more rapidly than by the conventional method using EPMA.[23,25] The purpose of this study is to establish a method to identify calcium aluminate inclusions in Ca treated Al-killed steel using CL analysis by analysing their CL images and CL spectra.

II. EXPERIMENTAL

CL analysis of calcium aluminate inclusions in Ca treated Al-killed steel was performed for model samples prepared by melting iron (Fe) with pure metals of Al and Ca in an argon atmosphere. This preparation method is the general procedure for model samples of steels containing nonmetallic inclusions in laboratory scale experiments. Electrolytic Fe powder (purity: 99.9%, Wako Pure Chemical Industries, Ltd., Osaka, Japan), Al powder (purity: 99.9%, Nacalai Tesque, Inc., Kyoto, Japan), and Ca shot (purity: 99.5%, The Nilaco Corporation, Tokyo, Japan) were placed in an Al_2O_3 crucible in various ratios, as shown in Table I. Sample A and B were prepared to obtain Al-rich calcium aluminate inclusions such as $CaAl_2O_4$, $Ca_3Al_{10}O_{18}$, $CaAl_4O_7$, and $CaAl_{12}O_{19}$, and Al_2O_3. Sample C was prepared to expect the formation of Ca-rich calcium aluminate inclusions such as $Ca_3Al_2O_6$ and $Ca_{12}Al_{14}O_{33}$. The mixture was heated at 1550 °C for 20 min and then cooled to room temperature in a flowing argon atmosphere (flow rate: 200 mL min^{-1}). Oxide layer on the Fe powder and residual oxygen in the argon gas contribute to the formation of inclusions of the samples. The surfaces of the samples were polished using 1200- and 2400-grid abrasive papers. The surfaces were then finished using a 1-μm diamond paste. We performed CL analysis of the model samples using a custom scanning electron microscope-cathodoluminescence (SEM-CL) system. Details of the SEM-CL system have been reported previously.[22,23] We briefly summarize the main points here. CL images of the samples were captured using a digital single-lens reflex camera (α7RII, Sony Corp., Tokyo, Japan) equipped with a zoom lens (LZM-06075A, Seimitu Wave Inc., Kyoto, Japan) through a quartz viewport attached to a commercial SEM instrument (Mighty-8DXL, TECHNEX, Tokyo, Japan). The sensitivity range of the camera was in the wavelength range from 420 to 680 nm. CL spectra of the samples were collected using an optical spectrometer (QE65Pro, Ocean Optics Inc., Florida, USA) by attaching a flange to introduce an optical fiber with a

collector lens (LGL-30, Chuo Precision Industrial Co., Ltd, Tokyo, Japan) on its forehead into the SEM chamber and connecting the optical fiber to the optical spectrometer. The measurement durations for the CL spectra were set to 100 s. Elemental analysis of the samples was also carried out using an SEM (S-3400N, Hitachi High-Technologies Co., Tokyo, Japan) equipped with a lithium-drifted silicon (Si (Li)) EDX detector (EDAX Inc., New Jersey, USA).

Table I. Compositions of model samples.

Sample	Fe (mass%)	Al (mass%)	Ca (mass%)
A	98	1.3	0.7
B	98	1.1	0.9
C	97	0.1	2.9
D	98	1.0	1.0

III. Results

Six types of calcium aluminates, $Ca_3Al_2O_6$, $Ca_{12}Al_{14}O_{33}$, $CaAl_2O_4$, $Ca_3Al_{10}O_{18}$, $CaAl_4O_7$, and $CaAl_{12}O_{19}$, have been reported in the CaO-Al_2O_3 system.[8-10,26,27] We collected the CL images and CL spectra of various calcium aluminate inclusions in the model samples to identify these calcium aluminate inclusions by CL analysis. The model samples were prepared by heating a mixture of Fe, Al, and Ca metals at 1550 °C under an argon atmosphere. The compositions of the calcium aluminate inclusions, whose CL images and CL spectra were obtained, were determined by SEM-EDX analysis. Figure 2(a) and (b) show a CL image and the corresponding SEM image, respectively, of an inclusion in Sample A. Almost the inclusion was removed by the polishing and an inclusion remained in the lower right of the rough area in Fig. 2(b). The remaining inclusion emitted blue luminescence and was confirmed to be $CaAl_2O_4$ (Ca: 32 at.%, Al: 68 at.%) by EDX point analysis. This luminescence color was consistent with the CL spectrum of the $CaAl_2O_4$ inclusion shown in Fig. 2(c) because the CL spectra showed a broad peak at around 450 nm. We also detected an

inclusion emitting blue-green luminescence in the upper area (Area 1) and blue-violet in the lower area (Area 2) in Sample A, as shown in Fig. 3(a). The corresponding SEM image is shown in Fig. 3(b). The CL image implied that the compositions of Areas 1 and 2 were different. This was confirmed by the EDX mapping of Ca in the areas as shown in Fig. 3(c) because the difference in the intensities of the Ca Kα line mostly corresponded to the areas emitting blue-green and blue-violet luminescence. The distribution of the intensities of the Ca Kα line seemed to be uniform in each region of Areas 1 and 2. The compositions of Areas 1 and 2 were confirmed to be $CaAl_4O_7$ (Ca: 20 at.%, Al: 80 at.%) and $Ca_3Al_{10}O_{18}$ (Ca: 26 at.%, Al: 74 at.%), respectively, by EDX point analysis. Therefore, $CaAl_4O_7$ and $Ca_3Al_{10}O_{18}$ inclusions emitted blue-green and blue-violet luminescence, respectively. Although CL spectra of the $CaAl_4O_7$ and $Ca_3Al_{10}O_{18}$ inclusions (Fig. 3(d)) showed that the intensities of a peak at around 675 nm (red to infrared) were higher than those at around 510 (blue-green) or 425 nm (blue-violet), neither $CaAl_4O_7$ or $Ca_3Al_{10}O_{18}$ inclusions emitted red luminescence. This was because the sensitivity of the digital camera around 675 nm was lower than that around 425 or 510 nm. The CL peak of the $CaAl_4O_7$ inclusion at 675 nm was consistent with the spectrum reported in previous studies[28,29] and originated from manganese (IV) ions (Mn^{4+}) substituting tetrahedrally coordinated aluminum (III) ions (Al^{3+}).[28,29] The Mn ions in the $CaAl_4O_7$ inclusion came from the Fe powder which was confirmed to contain 5 ppm of Mn.[24] An inclusion emitting red luminescence was also detected in the CL image of Fig. 3(a) (Area 3). The inclusion was identified to be Al_2O_3 by EDX point analysis. The CL peak of the Al_2O_3 inclusion at 745 nm, shown in Fig. 3(c), was in good agreement with that in previous reports.[23,30-32] The CL peak at 745 nm originated from titanium (III) ions (Ti^{3+}) substituting octahedrally coordinated Al^{3+}.[30-32] The Ti ions in the Al_2O_3 inclusion came from the Al_2O_3 crucible which was confirmed to contain 40 ppm of Ti.[24] The area intensity of the red region (620-680 nm) was one order magnitude higher than those of the other color regions. Thus, the

Al_2O_3 inclusion emitted red luminescence. Fig. 3(a) indicates that we can simultaneously distinguish $CaAl_4O_7$, $Ca_3Al_{10}O_{18}$, and Al_2O_3 inclusions by capturing their CL images.

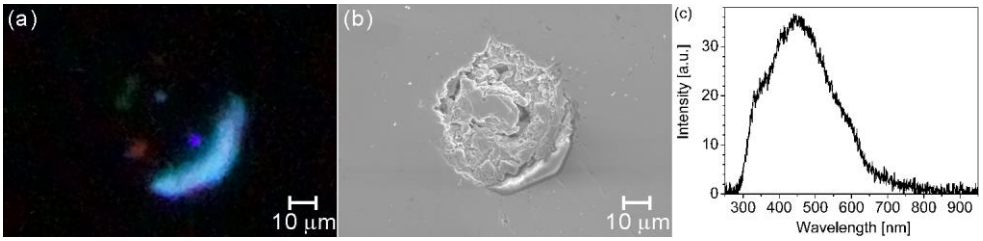

Fig. 2–(a) CL and (b) SEM images of an inclusion particle on the polished surface of sample A. The exposure time for the CL image was 2 s. (c) CL spectrum of the luminescent area in Fig. 2(a).

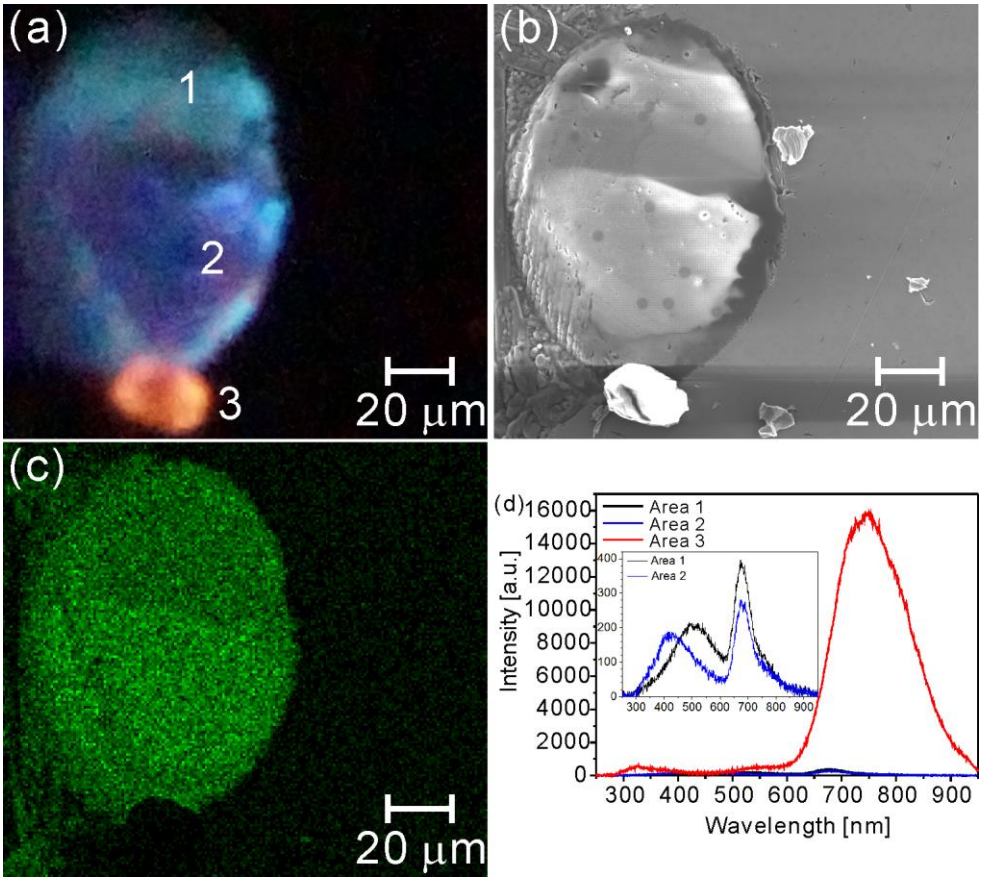

Fig. 3–(a) CL and (b) SEM images, and (c) EDX elemental mapping of Ca in another area of the polished surface of sample A. The exposure time for the CL image was 1 s. (d) CL spectra of Areas 1, 2, and 3 in Fig. 3(a). Enlarged CL spectra near the peaks of Areas 1 and 2 are shown in the upper left.

Figure 4(a) and (b) show a CL image and the corresponding SEM image, respectively, of an inclusion in Sample B. We detected a region emitting mainly three types of luminescence colors: blue-violet (Area 4), violet (Area 5), and blue-green (Area 6), which suggested the existence of three kinds of compounds. This result could also be inferred from the EDX mapping of Ca in the region, as shown in Fig. 4(c), because the distribution of the intensities of the Ca Kα line roughly agreed with that of the CL colors (Fig. 4(a)). The areas emitting violet (Area 5), blue-green (Area 6), and blue-violet (Area 4) corresponded to those with lower, medium, and higher intensities of the Ca Kα line, respectively. It should, however, be noted that the intensity of the Ca Kα line in the region was distributed to be somewhat non-uniform in comparison with that shown in Fig. 3(c). EDX point analysis revealed that the compositions of Areas 4, 5, and 6 were close to $CaAl_2O_4$ (Ca: 33 at.%, Al: 67 at.%), $CaAl_{12}O_{19}$ (Ca: 7 at.%, Al: 93 at.%), and $CaAl_4O_7$ (Ca: 21 at.%, Al: 79 at.%), respectively. The CL spectra of Areas 4, 5, and 6 are shown in Fig. 4(d). The spot size of the electron beam was approximately 20 μm during the measurement. The CL spectrum of Area 5 directly resulted in the violet luminescence because the CL peak appeared at 380 nm. It was inferred that the CL spectrum of Area 5 would be derived from that of $CaAl_{12}O_{19}$ because its spectral shape was completely different from the other calcium aluminates shown in Fig. 2(c), 3(d), and 5(c). The CL color and CL spectrum of Area 6 were almost identical with those of Area 1 in Fig. 3, which indicated that Area 6 consisted of $CaAl_4O_7$. In contrast, the CL color and CL spectrum of Area 4 were slightly different from those of $CaAl_2O_4$ shown in Fig. 2. The CL peak of Area 4 was located at 400 nm, which was 50 nm lower than that of $CaAl_2O_4$ shown in Fig. 2. Considering the slight non-uniform distribution of Ca in Area 4, the spot size of the electron beam, and the CL spectrum of $CaAl_{12}O_{19}$ with an intensity one order of magnitude higher than $CaAl_2O_4$, it was proposed that a small amount of $CaAl_{12}O_{19}$ co-existed in Area 4 and that the luminescence color in Area 4 was the mixed colors of $CaAl_2O_4$ and $CaAl_{12}O_{19}$.

Although some difficulties in the interpretation of the CL image and CL spectra would arise in non-uniformly distributed calcium aluminates inclusions, we found that capturing the CL image enabled $CaAl_2O_4$, $CaAl_4O_7$, and $CaAl_{12}O_{19}$ to be identified.

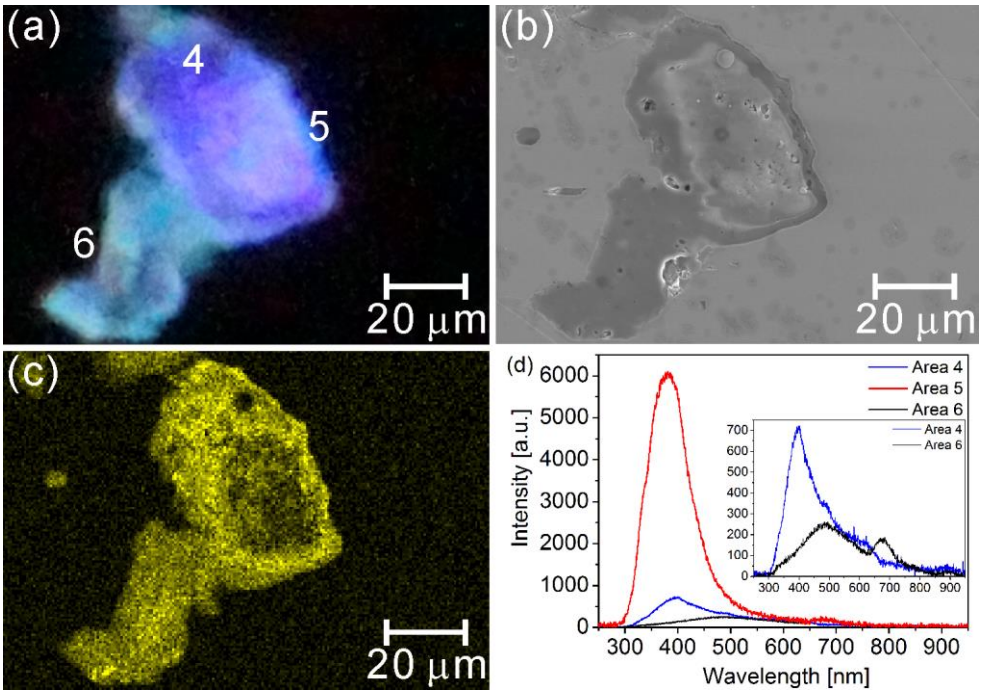

Fig. 4–(a) CL and (b) SEM images, and (c) EDX elemental mapping of Ca of the polished surface of sample B. The exposure time for the CL image was 1 s. (d) CL spectra of Areas 4, 5, and 6 in Fig. 4(a). Enlarged CL spectra near the peaks of Areas 4 and 6 are shown in the upper right.

$Ca_{12}Al_{14}O_{33}$ (Ca: 41 at.%, Al: 59 at.%) inclusions were detected in Sample C by EDX point analysis. The CL image and the corresponding SEM image of the $Ca_{12}Al_{14}O_{33}$ inclusion are shown in Fig. 5(a) and 5(b), respectively. The $Ca_{12}Al_{14}O_{33}$ inclusion emitted blue luminescence. This result was well supported by the CL spectrum of the $Ca_{12}Al_{14}O_{33}$ inclusion shown in Fig. 5(c) because the CL peak was located at around 470 nm. We were not able to prepare a sample containing $Ca_3Al_2O_6$ inclusions because calcium was easily vaporized from the sample. This suggested that it is difficult for $Ca_3Al_2O_6$ inclusions to be formed during Ca treatment in the steelmaking process. Actually, it has been reported that the formation of $Ca_3Al_2O_6$ inclusions was not confirmed in Ca treated Al-killed steels.[6]

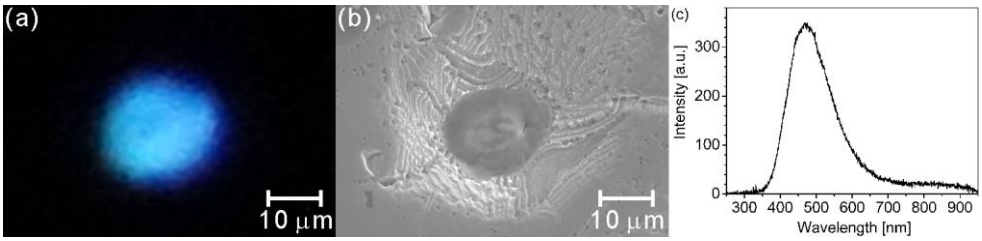

Fig. 5–(a) CL and (b) SEM images of an inclusion particle on the polished surface of sample C. The exposure time for the CL image was 1 s. (c) CL spectrum of the luminescent area in Fig. 5(a).

There have been no previous reports for identifying CL peaks of the calcium aluminates acquired in the present study except for the peaks of $CaAl_4O_7$ at 675 nm and of Al_2O_3 at 745 nm. It was considered from the compositional similarity to $CaAl_4O_7$ that the CL peak of $Ca_3Al_{10}O_{18}$ at 675 nm might arise from Mn^{4+}. The other unidentified CL peaks might be related to oxygen vacancies because CL peaks related to oxygen vacancies have been reported at around 335, 415, 480, and 540 nm for Al_2O_3[23,30-33] and at around 380 nm for CaO.[34] In addition, it has been reported that blue emission of glasses containing Al_2O_3 and CaO was related to oxygen vacancies.[35] The CL peaks of the inclusions detected in the present study are summarized in Table II.

Table II. Wavelength and luminescence center of CL peaks for inclusions detected in the present study.

Compound	Wavelength [nm]	Luminescence center
$Ca_{12}Al_{14}O_{33}$	470	Oxygen vacancy*
$CaAl_2O_4$	450	Oxygen vacancy*
$Ca_3Al_{10}O_{18}$	425	Oxygen vacancy*
	675	Mn^{4+} *
$CaAl_4O_7$	510	Oxygen vacancy*
	675	Mn^{4+} [28,29]
$CaAl_{12}O_{19}$	380	Oxygen vacancy*
Al_2O_3	745	Ti^{3+} [23,30-32]
CaS	580	Mn^{2+} [36-38]

* The luminescence center was speculated from previous reports.

It is known that CaS inclusions are formed in Ca treated Al-killed steels.[6,7] Thus, the CL image and CL spectrum of CaS inclusion are also important data for the analysis of nonmetallic inclusions in this type of steel. We detected a CaS inclusion in Sample D, and the CaS inclusion emitted yellow luminescence as shown in Fig. 6(a). The CL spectrum of the CaS inclusion showed a peak at 580 nm (Fig. 6(c)), which was consistent with that reported in previous studies.[36-38] Therefore, the luminescence color of the CaS inclusion arose from the peak at 580 nm. The CL peak was considered to originate from Mn^{2+} substituting Ca^{2+}.[36-38] The peak position of the CaS inclusion did not overlap with that of the calcium aluminates prepared in the present study. Therefore, it was expected that a CaS inclusion in Ca treated Al-killed steels is distinguishable by capturing the CL image.

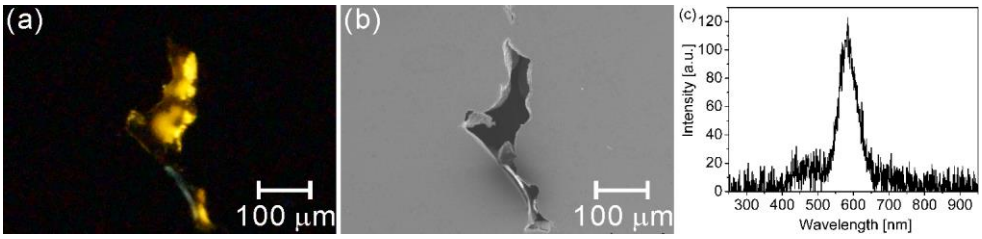

Fig. 6–(a) CL and (b) SEM images of an inclusion particle on the polished surface of sample D. The exposure time for the CL image was 10 s. (c) CL spectrum of the luminescent area in Fig. 6(a).

IV. DISCUSSION

We successfully obtained the CL images and CL spectra of $Ca_{12}Al_{14}O_{33}$, $CaAl_2O_4$, $Ca_3Al_{10}O_{18}$, $CaAl_4O_7$, $CaAl_{12}O_{19}$, and Al_2O_3 inclusions in the model samples. These findings provide insight for distinguishing $Ca_{12}Al_{14}O_{33}$, $CaAl_4O_7$, $CaAl_{12}O_{19}$, and Al_2O_3 inclusions, which lead to nozzle clogging and melting of the stopper rod, from $Ca_3Al_{10}O_{18}$ and $CaAl_2O_4$ inclusions, which do not cause such problems. Fig. 3, 4, and 5 suggest that $Ca_{12}Al_{14}O_{33}$, $CaAl_4O_7$, $CaAl_{12}O_{19}$, and Al_2O_3 inclusions can be distinguished from a $Ca_3Al_{10}O_{18}$ inclusion by capturing CL images and CL spectra. This is because the luminescence colors of $Ca_{12}Al_{14}O_{33}$ (blue), $CaAl_4O_7$ (blue-green), $CaAl_{12}O_{19}$ (violet), and Al_2O_3 (red) inclusions are

different from that of $Ca_3Al_{10}O_{18}$ (blue-violet) inclusion. Comparing Fig. 2(a), 3(a), and 4(a) indicates that $CaAl_4O_7$, $CaAl_{12}O_{19}$ and Al_2O_3 inclusions are also distinguishable from a $CaAl_2O_4$ inclusion by their CL colors because the $CaAl_2O_4$ inclusion emitted blue luminescence. It should be noted that the area consisting of $CaAl_{12}O_{19}$ and $CaAl_2O_4$ inclusions emitted mixed violet and blue luminescence as shown in Fig. 4(a), which was proposed from the CL spectra of the area (Fig. 4(d)), $CaAl_{12}O_{19}$ inclusion (Fig. 4(d)), and $CaAl_2O_4$ inclusion (Fig. 3(d)). In contrast, it was difficult to distinguish a $Ca_{12}Al_{14}O_{33}$ inclusion from a $CaAl_2O_4$ inclusion owing to their similar CL colors, as shown in Fig. 2(a) and 5(a). Fig. 2(c) suggests that $CaAl_2O_4$ inclusion has CL intensities in a wavelength range from 300 nm to 420 nm, which is out of the sensitivity range of the camera. This indicates that we can identify $Ca_{12}Al_{14}O_{33}$ and $CaAl_2O_4$ inclusions from their CL colors if we use a camera in which the built-in filter is removed. The built-in filter prevents ultraviolet and infrared light from entering into the CMOS sensors in the camera. The sensitivity range of the camera would extend to 350–1000 nm by detaching the built-in filter.[39] We observed a clear difference in the CL color between $Ca_{12}Al_{14}O_{33}$ and $CaAl_2O_4$ inclusions using the camera without the built-in filter, as shown in Fig. 7. We were unable to confirm the area emitting red luminescence in Fig. 7(a) by EDX point analysis because the inclusion particle was too small to detect the characteristic X-rays from the inclusion alone. We also were unable to acquire the corresponding CL spectrum owing to the low intensity. It could be inferred from the CL spectra of calcium aluminate inclusions obtained in the present study that the red luminescence might originate from Al_2O_3 inclusion because of its high CL intensity in the red color region. The exposure times for all the CL images in the present study were less than 10 s, which was shorter than the measurement duration using EPMA. Therefore, our results provide a method to rapidly identify the calcium aluminate inclusions, which lead to nozzle clogging and melting of the stopper rod by CL analysis. In real conditions, Ca treated Al-

killed steels contain $MgAl_2O_4$ spinel including other elements in addition to calcium aluminate inclusions and CaS inclusion.[6,27,40] Future work should focus on the identification of the calcium aluminate inclusions which cause neither nozzle clogging or melting of the stopper rod in actual Ca treated Al-killed steels. It should be noted that capturing CL would contribute to the rapid identification of separated calcium aluminate inclusions but might be difficult for the identification of an agglomerated inclusion consisting of calcium aluminates with several compound forms owing to the overlap of their luminescence. In this case, acquiring CL spectra would help in the identification of such inclusions, as described in Fig. 4, although the acquisition time would be increased to approximately a few minutes.

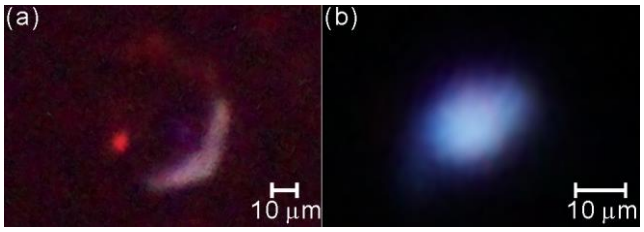

Fig. 7–CL images of (a) $CaAl_2O_4$ and (b) $Ca_{12}Al_{14}O_{33}$ inclusions using the camera without the built-in filter. The captured areas of (a) and (b) are the same as those in Fig. 2(a) and Fig. 5(a), respectively. The exposure time was 5 s, each.

V. CONCLUSIONS

This study focuses on establishing a CL analytical method to distinguish calcium aluminate inclusions of $Ca_{12}Al_{14}O_{33}$, $CaAl_4O_7$, $CaAl_{12}O_{19}$, and Al_2O_3 in steels, which lead to nozzle clogging and melting of the stopper rod during continuous casting, from those of $CaAl_2O_4$ and $Ca_3Al_{10}O_{18}$ in steels, which do not cause such problems. We acquired the CL images and CL spectra of calcium aluminate inclusions in mixtures of Fe powder, Al powder, and Ca shot heated at 1550 °C in an argon atmosphere. The $CaAl_2O_4$ inclusion emitted blue luminescence owing to a CL peak at 450 nm. The $Ca_3Al_{10}O_{18}$ inclusion emitted blue-green luminescence and showed CL peaks at 510 and 675 nm. The $Ca_3Al_{10}O_{18}$ inclusion could be distinguished from the calcium aluminate inclusions that lead to the problems during

continuous casting by their CL colors because $Ca_{12}Al_{14}O_{33}$, $CaAl_4O_7$, $CaAl_{12}O_{19}$, and Al_2O_3 inclusions emit blue luminescence with a CL peak at 470 nm, blue-violet with CL peaks at 425 and 675 nm, violet with a CL peak at 380 nm, and red with a CL peak at 745 nm, respectively. We could also identify the $CaAl_2O_4$ inclusion from $CaAl_4O_7$, $CaAl_{12}O_{19}$, and Al_2O_3 inclusions by their CL colors. However, it was difficult to distinguish the $CaAl_2O_4$ inclusion from the $Ca_{12}Al_{14}O_{33}$ inclusion owing to their similar CL colors. This difficulty was solved by using a digital camera without the built-in filter, which removed luminescence at wavelengths below 420 nm and above 680 nm. This was because the $CaAl_2O_4$ inclusion has relatively higher CL intensities in the ultraviolet region (350–420 nm) than the $Ca_{12}Al_{14}O_{33}$ inclusion. We also acquired the CL image and CL spectrum of the CaS inclusion. CaS emitted yellow luminescence with a CL peak at 580 nm which did not overlap with the CL peaks of the calcium aluminate inclusions prepared in this study. These results indicate that the CaS inclusion is distinguishable from calcium aluminate inclusions in Ca treated Al-killed steels. The acquisition times for the CL images were less than 10 s. Therefore, the method we present in the present study has potential for the rapid identification of calcium aluminate inclusions in steels, which would contribute to an actual control of the operation in steel-making production. To identify calcium aluminates in agglomerated inclusions with several compositions, a spectroscopic analysis of the CL spectra would provide more detailed information than the CL image itself.

ACKNOWLEDGEMENTS

This work was supported by JSPS KAKENHI [Grant Numbers 17H03435].

REFERENCES

1. H. Suito, R. Inoue R: *ISIJ Int.*, 1996, vol. 36, pp. 528–36.
2. L. Zhang, B. G. Thomas: *ISIJ Int.*, 2003, vol. 43, pp. 271–91.
3. H. V. Atkinson, G. Shi: *Prog. Mater. Sci.*, 2003, vol. 48, pp. 457–520.
4. L. Zhang, B. G. Thomas: *Metall. Trans.B*, 2006, vol. 37B, pp. 733–61.
5. E. T. Turkdogan: *Fundamentals of steelmaking*, Institute of Metals, London, 1996, pp. 285–94.
6. S. Abdelaziz, G. Megahed, L. El-Mahallawi, H. Ahmed: *Ironmak. Steelmak.*, 2009, vol. 36, pp. 432–41.
7. M. Lind, L. Holappa: *Metall. Trans. B*, 2010, vol. 41B, pp. 359–66.
8. Nippon Steel Corp, Y. Kinomoto, H. Hayashi, H. Ishii: *Erosion prevention method of stopper for continuous casting*, JP 07-223058 A, 1995-08-22.
9. Y. Kusano, Y. Kawauchi, M. Wajima, K. Sugawara, M. Yoshida, H. Hayashi: *CAMP-ISIJ*, 1995, vol. 8, pp. 59–62.
10. S. Kimura: *Secondary smelting / special melting, in: Handbook of Iron and Steel*, vol. 1, 5th ed., The Iron and Steel Institute of Japan, Tokyo, 2014, pp. 373.
11. M. Fernandes, J. C. Pires, N. Cheung, A. Garcia: *Mater. Charact.*, 2003, vol. 51, pp. 301–8.
12. M. Onodera, M. Saeki, K. Nishizaka, T. Sakata, J. Ono, I. Fukui, N. Imamura: *Tetsu To Hagane–J. Iron Steel Inst. Jpn.*, 1974, vol. 60, pp. 2002–12.
13. H. Falk, P. Wintjens: *Spectrochim. Acta B*, 1998, vol. 53, pp. 49–62.
14. Y. Nuri, K. Umezawa: *Tetsu To Hagane–J. Iron Steel Inst. Jpn.*, 1989, vol. 75, pp. 1897–1904.
15. K. C. Mills, P. N. Questede, R. F. Brooks, D. M. Hayes: *Proc. Ethem T. Turkdogan Symp.*, 1994, pp. 105–111.
16. H. Kondo, T. Toh, R. Uemoto, T. Suzuki, K. Chiba, H. Yamamura, M. Wakoh, E. Takeuchi: *Tetsu To Hagane–J. Iron Steel Inst. Jpn.*, 2003, vol. 89, pp. 1000–04.
17. H. Hocquaux, R. Meilland,: *Rev. Metall.*, 1992, vol. 12, pp. 193–99.
18. R. Noll, H. Bette, A. Brysch, M. Kraushaar, I. Mönch, L. Peter, V. Sturm: *Spectrochim. Acta B*, 2001, vol. 56, pp. 637–49.
19. H. Yin, H. T. Tsai: *Proc. ISS Tech Conf.*, 2003, pp. 217–226.
20. P. Kaushik, H. Pielet, H. Yin: *Ironmak. Steelmak.*, 2009, vol. 36, pp. 572–82.
21. H. Kondo: *Tetsu To Hagane–J. Iron Steel Inst. Jpn.*, 2004, vol. 90, pp. 758–65.
22. S. Imashuku, K. Ono, K. Wagatsuma: *X-Ray Spectrom.*, 2017, vol. 46, pp. 131–35.
23. S. Imashuku K. Ono, R. Shishido, S. Suzuki, K. Wagatsuma: *Mater. Charact.*, 2017, vol. 131, pp. 210–16.
24. S. Imashuku, K. Ono, K. Wagatsuma: *Microsc. Micoanal.*, 2017, vol. 23, pp. 1143–49.
25. S. Imashuku, K. wagatsuma: *Sur. Interface Anal.*, 2018, accepted.
26. K. Narita: *Tetsu To Hagane–J. Iron Steel Inst. Jpn.*, 1966, vol. 52, pp. 1098–145.
27. J. Lamut, J. Falkus, B. Jurjevec, M. Knap: *Arch. Metall. Mater.*, 2012, vol. 57, pp. 319–24.
28. J. Park, G. Kim, Y. J. Kim: *Ceram. Int.*, 2013, vol. 39, pp. S623–26.
29. P. Li, M. Peng, X. Yin, Z. Ma, G. Dong, Q. Zhang, J. Qiu: *Opt. Express*, 2013, vol. 21 pp. 18943–48.
30. P. D. Townsend, A. P. Rowlands: *Information Encoded in Cathodoluminescence Emission Spectra, in: Cathodoluminescence in Geoscience*, Springer, Berlin, 2000, pp. 41–57.
31. M. Gaft, R. Resfeld, G. Panczer: *Modern Luminescence Spectroscopy of Minerals and Materials*, Springer, Berlin, 2005, pp. 95–96.

32. M. Ghamnia, C. Jardin, M. Bouslama: *J. Electron Spectrosc. Relat. Phenom.*, 2003, vol. 133, pp. 55–63.
33. M. Karakus, R. E. Moore: *Am. Ceram. Soc. Bull.*, 1998, vol. 77, pp. 55–61.
34. B. Henderson, S. E. Stokowski, T. C. Ensign, *Phys. Rev.*, 1969, vol. 183, pp. 826–831.
35. A. Novatski, A. Steimacher, A. N. Medina, A. C. Bento, M. L. Baesso, L. H. C. Andrade, S. M. Lima, Y. Guyot, G. Boulon: *J. Appl. Phys.*, 2008, vol. 104, pp. 094910.
36. S. Asano, N. Yamashita, M. Oishi,: *J. Phys. Soc. Jpn.*, 1968, vol. 25, pp. 789–98.
37. N. Yamashita, S. Maekawa, K. Nakamura: *Jpn. J. Appl. Phys.*, 1990, vol. 29, pp. 1729–32.
38. N. Ruelle, M. Pham-Thi, C. Rouassier: *J. Appl. Phys.*, 1992, vol. 31, pp. 2786–90.
39. https://astronomy-imaging-camera.com/products/asi-cooled-cameras/asi094mc-pro-color/ Accessed 17 April 2018
40. W. Yang, L. Zhang, X. Wang, Y. Ren, X. Liu, Q. Shan, *ISIJ Int.*, 2013, vol. 53, pp. 1401–10.

380 **Table I.** Compositions of model samples.

Sample	Fe (mass%)	Al (mass%)	Ca (mass%)
A	98	1.3	0.7
B	98	1.1	0.9
C	97	0.1	2.9
D	98	1.0	1.0

381

Table II. Wavelength and luminescence center of CL peaks for inclusions detected in the present study.

Compound	Wavelength [nm]	Luminescence center
$Ca_{12}Al_{14}O_{33}$	470	Oxygen vacancy*
$CaAl_2O_4$	450	Oxygen vacancy*
$Ca_3Al_{10}O_{18}$	425	Oxygen vacancy*
	675	Mn^{4+} *
$CaAl_4O_7$	510	Oxygen vacancy*
	675	Mn^{4+} [28,29]
$CaAl_{12}O_{19}$	380	Oxygen vacancy*
Al_2O_3	745	Ti^{3+} [23,30-32]
CaS	580	Mn^{2+} [36-38]

* The luminescence center was speculated from previous reports.